Hydromorphological Monitoring and Navigation Assessment on Alluvial River Sections Using Sentinel-2 and Water Gauge Data

Michał Śmiarowski [1]

[1] Department of Imagery Intelligence, Faculty of Civil Engineering and Geodesy, Military University of Technology, 2 Gen. S. Kaliskiego Street, Warsaw, Poland – michal.smiarowski@wat.edu.pl

Keywords: Sentinel-2, Sandbar mapping, Water gauge data, Inland navigation, Hydromorphological change, River morphology.

Abstract

Monitoring dynamic alluvial rivers is essential for safe inland navigation, yet traditional bathymetric surveys are costly and infrequent. This paper presents an automated method for detecting migrating sandbars by integrating Sentinel-2 satellite imagery with daily water gauge data. Implemented in Google Earth Engine (GEE), the algorithm matches specific water levels with cloud-optimized images to map emerging shoals. Water and sediment were separated using the Sentinel Water Mask (SWM) index, while a 30-meter internal channel buffer mitigated shoreline mixed-pixel errors. The method’s accuracy was validated using 3-meter resolution PlanetScope imagery. Results demonstrated high geometric agreement (mean Intersection over Union = 0.71) and a strong area correlation (R^2 = 0.97). Notably, the 10-meter Sentinel-2 resolution caused a systematic 26% overestimation of sandbar size. However, for navigation, this overestimation provides a beneficial safety margin that prevents the underestimation of submerged obstacles. By correlating specific gauge levels with sandbar emergence, the extracted 2D contours provide a vital spatial baseline that enables the future estimation of available water columns over specific bottlenecks. Ultimately, this cost-effective procedure allows for the continuous generation of spatial databases, forming a practical foundation for dynamic relative depth mapping within River Information Services (RIS).

1. Introduction

Contemporary management of alluvial waterways requires a transition from traditional, costly, and point-based bathymetric measurements toward continuous monitoring systems based on satellite data. Rivers with high morphological dynamics, which includes the Vistula in Poland, are characterized by intense sediment transport, leading to constant changes in channel configuration. These phenomena have a direct impact on navigation safety, determining the availability of the so-called Safe Navigation Layer (SNL).

A significant factor modifying the Vistula’s channel processes was the 19th- and 20th-century river regulation carried out between 1856-1878 and 1900-1914 on the section from the Russian-Prussian border to the Gulf of Gdańsk (Babiński, 1992). The regulation works, involving the construction of over 2100 km of longitudinal dams and nearly 600 groynes, aimed to narrow the channel to a designed width of 375 meters for an average flow. Before regulation, the average channel width on the 719-814 km section was 785 meters, which means that technical intervention reduced the space for water flow and sediment transport by almost half (Kryniecka and Magnuszewski, 2021). The construction of groynes ranging from several to several hundred meters in length, perpendicular to the channel banks, contributed to changes in the river’s hydrodynamic conditions. Changes occurred in the course of the mainstream and river currents, and consequently, this hydrotechnical development led generally to two directions of channel process development: erosional and accumulative (Babiński, 1992). The result of the regulatory processes was the forcing of the river flow within its established channel, which, under conditions of high bedload supply reaching from 0.7 to 1.0 million m^3 annually, led to the formation of a specific system of channel mesoforms such as lateral bars and middle-central bars (Habel, 2013). From the perspective of hydrology and navigation, these accumulative forms constitute the primary obstacle in waterway exploitation and threaten navigation safety on the international waterways E40 and E70 (Schoeneich et al., 2022; Woś, 2017). As research indicates (Pieron et al., 2013), the lower Vistula is not currently a homogeneous system, which results, among other factors, from the presence of the Włocławek barrage, which permanently disrupted the continuity of sediment transport. Bedload transport is “unloaded” in areas of forced accumulation, creating complex systems of shoals with depths dropping below 1.0 meter during low-water periods (Office of the Marshal of the Pomorskie Voivodeship, 2026). The lack of up-to-date bathymetric data for many river sections makes assessing navigation feasibility extremely difficult. Despite the strategic importance of the Vistula, the management of its waterway encounters informational barriers. Bathymetric data are not available for many river stretches, and hydrometric data alone do not directly indicate the possibility of navigation.

Particularly problematic is the lower reach of the Vistula from the city of Grudziądz to the village of Biała Góra, which is classified as a class II navigable waterway with a transit depth of 1.6 m (Prime Minister, 2022). This section, being part of the international waterways E40 and E70, remains a high-risk navigation area in reality. Navigation on this segment is extremely demanding due to ubiquitous and dynamically migrating sandbars (Woś, 2017). Traditional river channel monitoring methods based on hydroacoustic techniques, such as multibeam echosounders - although precise - carry high operational costs and low temporal resolution, making it impossible to track short-term changes, e.g., after the passage of flood waves. In this context, satellite remote sensing techniques offer new possibilities. The use of the Sentinel-2 constellation, characterized by a spatial resolution of 10 meters and a temporal resolution of approximately 5 days, allows for the continuous monitoring of hydromorphological changes. Of particular importance is the application of the Sentinel Water Mask (SWM) index, optimized for turbid inland waters and bright alluvial sands, enabling precise separation of water from emerged sandbars (Kryniecka and Magnuszewski, 2020). By linking hydrometric data, specifically river gauge values, with satellite imagery from the Sentinel-2 constellation in defined time series, a reliable assessment of the river channel’s hydromorphological state becomes possible.

This paper presents a method for the automatic selection and processing of satellite data in the Google Earth Engine (GEE) environment and their correlation with water gauge data. The integration of these datasets allows for modeling the channel across varying water levels, which consequently provides the data necessary to create dynamic depth maps. Such an approach not only facilitates the assessment of current navigability on a shoal-strewn channel but also forms a foundation for the development of highly applicable River Information Services (RIS).

2. Study area and data

The study area (Figure 1) covers an approx. 55-kilometer stretch of the Lower Vistula, extending from Grudziądz (km 834) to Biała Góra (km 886). The selection of this research area stems from its strategic importance for water transport and the high morphological dynamics of the channel.

2.1 Hydrological and Navigation Characteristics

The studied section is part of the E40 and E70 international waterways. According to the AGN (European Agreement on Main Inland Waterways of International Importance) classification, it should meet the requirements of class IV navigability; however, in reality, it operates as a class II waterway with a guaranteed transit depth of 1.6 meters. In practice, these parameters are rarely achieved due to migrating shoals (Kotowska et al., 2019; Kubiak-Wójcicka and Manoiu, 2025; Prime Minister, 2022). The particular significance of this area arises from the fact that, navigating upstream from the mouth of the Vistula, it is the first section of a distinctively alluvial nature, characterized by the massive presence of morphological channel forms. While the channel below Biała Góra is relatively stable, the dynamics of sediment transport increase rapidly above the Biała Góra node (km 886.4). For inland navigation vessels moving upstream, the analyzed section thus constitutes the first critical navigation barrier, determining the feasibility of further transport deep into Poland's water system.

One water gauge station is located in the studied section in Grudziądz (km 834.5), for which the "0" elevation is 13.81 m a.s.l.. Due to the lack of active stations in the rest of the area of interest, this gauge was adopted as the reference station in the conducted research (the nearest downstream gauge is located in Tczew - km 908.6) (Monitoring Hydro - Hydrological Service of Poland [Serwis Hydrologiczny - Monitoring Hydro], 2026). The choice of the reference gauge is justified by the fact that Grudziądz marks the beginning of the analyzed section, where massive exposure of sandy channel forms occurs at low water levels. Based on water gauge data for Grudziądz and Tczew from July 2022 (Table 1), the longitudinal slope was calculated at 0.18 ‰ (i.e., 18 cm for every kilometer of the river). Therefore, the flow in this section is typical for lowland rivers in their lower reaches (Institute of Meteorology and Water Management - National Research Institute, 2022).

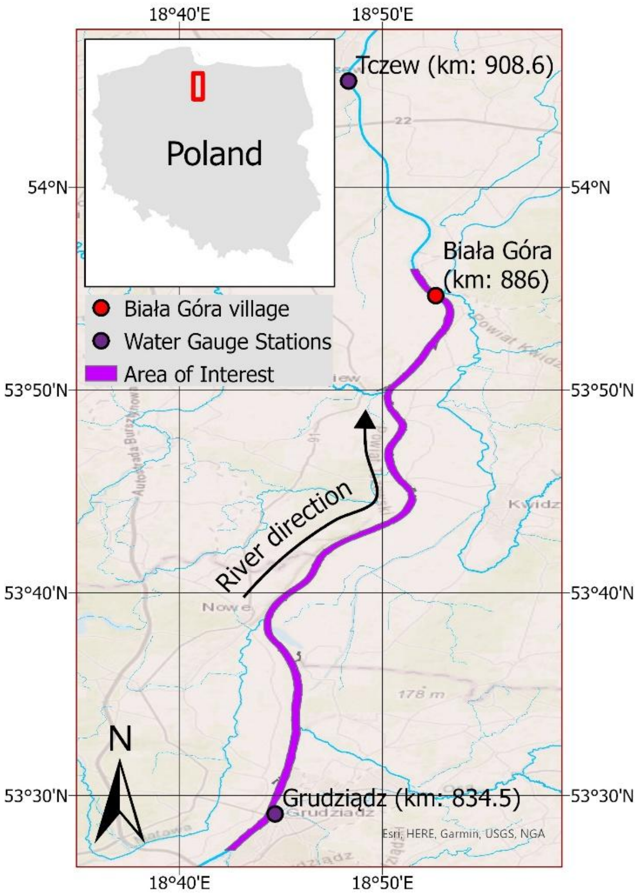

Figure 1. Location of the study area encompassing a 55-km section of the Lower Vistula River. The map illustrates the defined Area of Interest (AOI) alongside the reference water gauge station in Grudziądz. Basemap sources: Esri, HERE, Garmin, USGS.

Gauge Station	River [km]	Zero Gauge [m a.s.l.]	Min. Water Level [cm]	Water Surface Elevation. [m a.s.l.]
Grudziądz	834.50	13.99	151	15.50
Tczew	908.60	-0.50	240	1.90

Table 1. Water gauge data for the same day in July 2022 (Institute of Meteorology and Water Management - National Research Institute, 2022; Monitoring Hydro - Hydrological Service of Poland [Serwis Hydrologiczny - Monitoring Hydro], 2026).

This area is also important for ecological reasons, falling within the "Lower Vistula Valley" Natura 2000 zone. Studies concerning the availability of nesting habitats for birds indicate that the operations of the Włocławek barrage and frequent water level fluctuations negatively affect the stability of sandbars (Habel, 2018). This constitutes an additional argument for the necessity of monitoring them not only for navigation but also for environmental preservation.

2.2 Data

The research utilized a multi-source approach, integrating satellite data of varying spatial resolution, archival hydrometric data, and vector resources from the national geodetic and cartographic resource.

2.2.1 Satellite imagery - Sentinel-2 (Open Access): The primary data source for the analysis is imagery from the Sentinel-2 mission, implemented under the ESA Copernicus program. This mission is based on a pair of satellites orbiting on the same path, phased at 180° to each other, allowing for a high revisit frequency of 5 days at the equator. The satellites are equipped with an MSI optical instrument, recording images in 13 spectral bands with a resolution ranging from 10 to 60 meters. The research utilized Level-2A (L2A) products, which are orthorectified and georeferenced, including atmospheric correction and a Scene Classification (SCL) layer. The SCL layer enabled precise cloud filtering exclusively within the river channel area (AOI) ("Sentinel-2 Products Specification Document," 2025).

2.2.2 Validation imagery - PlanetScope (Planet Labs PBC): High-resolution data from the PlanetScope constellation, offered by Planet Labs PBC, were used as the standard of reference (ground truth). The study applied imagery from the SuperDove generation of satellites, which record images in eight spectral bands with a ground sample distance (GSD) of approx. 3.0 m. These data were acquired under a scientific license (Planet's Education and Research Program). The PlanetScope Ortho Analytic 8B SR (Level 3B) product was selected, characterized by Surface Reflectance and full radiometric correction. During the data ordering process, the Planet Harmonization tool was applied, transforming SuperDove spectral values into Sentinel-2 sensor equivalents, ensuring radiometric consistency between the sensors ("Technical Specification | Planet Documentation," 2026).

2.2.3 Hydrological data (IMGW-PIB): The temporal correlation of imagery relies on daily readings from the water gauge station in Grudziądz (km 834.5). The "0" elevation of the gauge is 13.81 m a.s.l. (Institute of Meteorology and Water Management - National Research Institute, 2022). These measurements served as the overarching filter for scene selection, allowing satellite acquisition dates to be matched to specific water surface elevations with a tolerance of ±0.15 m.

2.2.4 Vector data (BDOT10K): The Topographic Objects Database (BDOT10K) at a 1:10,000 scale enabled the optimization of the processing workflow. It was used to define a precise Area of Interest (AOI) mask covering only the Vistula river channel (Head Office of Geodesy and Cartography (GUGiK), 2025). Thanks to the BDOT10K mask, the entire image area was not indiscriminately analyzed for cloud cover or the presence of water. Limiting the algorithms' field of view exclusively to the interior of the channel allowed for the automatic elimination of spectral noise originating from riparian vegetation and coastal infrastructure, which significantly increased the reliability of the automated sandbar extraction results.

3. Methodology

The research methodology is based on a proprietary algorithm implemented in the Google Earth Engine (GEE) environment using the Python API in Google Colab. The process was designed as an automated technological pipeline, concluding with manual verification and a resulting database enabling visualizations in GIS software. The complete data processing pipeline, integrating Sentinel-2 imagery with water gauge data, is visually summarized in the flowchart in Figure 2.

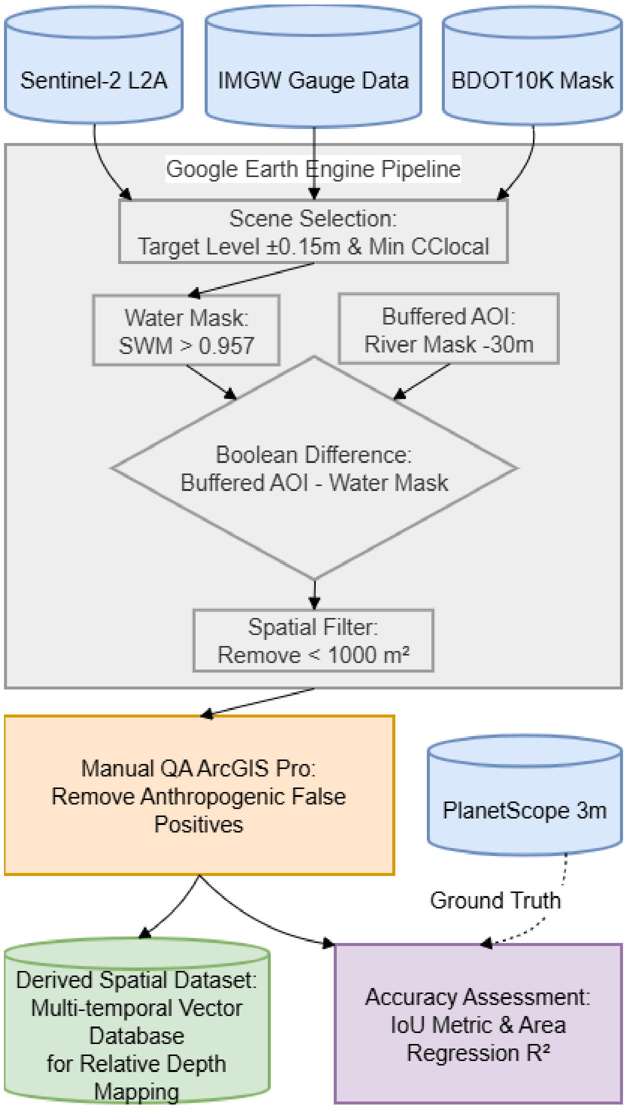

Figure 2. Flowchart of the proposed methodology. The process integrates Sentinel-2 imagery and gauge data within a Google Earth Engine pipeline, followed by manual quality assurance to produce a derived spatial dataset for relative depth mapping.

3.1 Hydrological Data Processing and Time Series Construction

The first stage involved selecting image dates based on daily IMGW-PIB data for the Grudziądz station (km 834.5). Due to the specifics of providing data in hydrological years (the hydrological year begins on November 1), an ETL (Extract, Transform, Load) procedure was implemented to adapt the data structure to calendar years. An important filtering criterion was the exclusion of river ice phenomena and the selection of days when the water level oscillated around defined intervals (every 0.5 m) with a tolerance of ±0.15 m. This allowed for obtaining a set of dates representative of specific morphological phases of the channel, ranging from low to medium states.

3.2 Image Selection and Cloud Optimization in GEE

The vector mask of the Vistula channel from the BDOT10K database was used as the spatial basis. Before its use, topology correctness was verified to ensure data completeness. The area prepared in this way was defined as the Area of Interest (AOI). The Sentinel-2 L2A image collection was filtered to extract

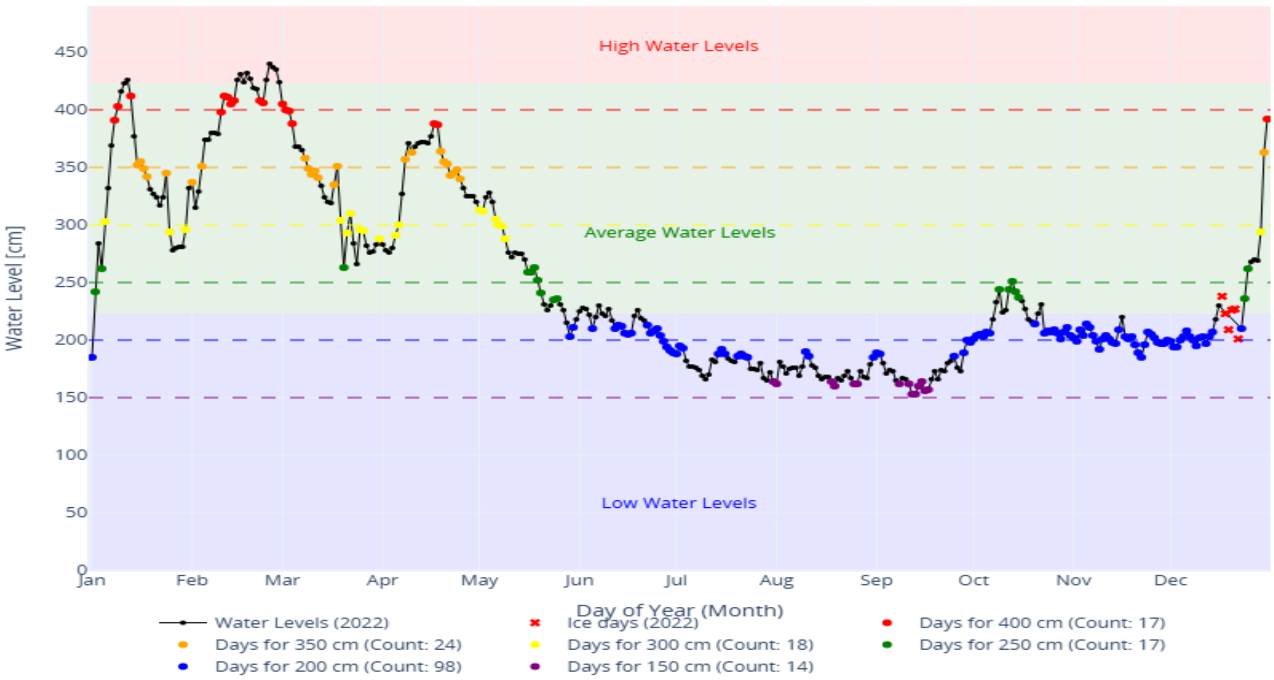

Figure 3. Annual hydrograph of the Vistula River at the Grudziądz gauge station (2022) illustrating the automated selection of Sentinel-2 imagery. Colored markers indicate successful image acquisitions synchronized with predefined water level contours.

scenes corresponding to the designated hydrological dates. A selection algorithm based on the local cloud cover index (CC_{local}) was implemented, calculated according to the formula:

$$CC_{local} = \frac{\sum_{i \in AOI} P_{cloudy}(i)}{\sum_{i \in AOI} P_{total}(i)} \times 100 \tag{1}$$

where: AOI - the area bounded by the vector mask of the Vistula channel from the BDOT10K database for the studied area,
$P_{cloudy}(i)$ - pixels classified in the SCL layer as high and medium probability clouds and cloud shadows (classes 3, 8, 9, 10),
$P_{total}(i)$ - total number of pixels inside the channel mask.

The application of this filter allowed for the use of images with low cloud cover directly over the river channel, even if the global cloud cover index for the entire scene showed a high level. Scenes with the lowest CC_{local} value for each specified water level were qualified for further processing. The selection results are presented in Table 2 and Figure 3.

Target Contour (Water Level) (±15 cm)	Matching Days (IMGW)	Found Sentinal-2 Scenes	Selected Date (YYYY-MM-DD)	Cloud Cover in AOI (%)
400 cm	17	12	2022-04-17	0.00%
350 cm	24	20	2022-03-08	0.00%
300 cm	18	18	2022-03-21	0.00%
250 cm	17	14	2022-10-12	5.89%
200 cm	98	72	2022-06-24	0.00%
150 cm	14	12	2022-09-12	30.28%

Table 2. Sample results of the automatic Sentinel-2 scene selection (year 2022) based on hydrological (water level ±15 cm) and meteorological (cloud cover in AOI) criteria.

3.3 Water Mask Extraction

For the selected images, the Sentinel Water Mask (SWM) index was calculated according to the formula:

$$SWM = \frac{B_{Blue} + B_{Green}}{B_{NIR} + B_{SWIR1}} = \frac{B2 + B3}{B8 + B11} \tag{2}$$

The separation of water from sandy sediments was carried out using a constant empirical threshold of $SWM_{THRESHOLD} = 0.957$ (Kryniecka and Magnuszewski, 2021, 2020). Pixels with values above the threshold were assigned to the "water" class, creating a binary mask of the filled channel.

3.4 Filtration and Mesoform Extraction

The actual sandbar extraction process was designed to minimize the impact of edge errors and spectral noise. To remove edge artifacts resulting from the mixed pixel effect at the land-water interface, the prepared channel mask (AOI) was subjected to a negative buffering operation of -30 meters. The application of a -30 m buffer (corresponding to the width of three Sentinel-2 sensor pixels) limited the influence of the signal from mixed pixels occurring at the shoreline, significantly increasing the spectral purity of the sample. The extraction logic was based on a set difference operation, identifying areas inside the buffered channel mask that were not classified as water by the SWM index:

$$M_{Sandbar} = M_{River\_Buffered} \setminus M_{Water\_Mask} \tag{3}$$

where: $M_{Sandbar}$ - the resulting binary mask of emerged sandbars,
$M_{River\_Buffered}$ - vector mask of the Vistula channel (BDOT10K) with the applied internal buffer,
M_{Water_Mask} - binary water mask obtained by thresholding the SWM index.

The raw extraction results were subjected to “salt-and-pepper” noise filtration using the *connectedPixelCount* algorithm. All objects whose continuous area was smaller than 10 pixels were removed from the analysis, which at Sentinel-2 resolution corresponds to an area of 1000 m². This ensured the elimination of artifacts resulting from water turbulence.
The binary mask was then processed into vector format (polygons) while maintaining the 10 m scale. Each polygon was automatically assigned metadata attributes:

- water_level_cm: the water surface elevation in Grudziądz corresponding to a given contour line,
- image_date: the calendar date of the Sentinel-2 image acquisition.

3.5 Manual Verification and Cleaning

The next stage was manual quality control performed in ArcGIS Pro software. Despite the high efficiency of automatic filtering, the raw vector results required additional correction to remove false-positive errors. This process involved the elimination of anthropogenic objects. Polygons detected on bridges, pillars of destroyed bridges remaining in the river current, power line networks, and hydrotechnical infrastructure (groynes) were removed from the database. Due to their high reflectivity or their circumvention of the negative edge buffer (-30 meters), these objects were incorrectly classified as sandy forms. Manual cleaning also included clearing areas affected by current cloud cover on data for the 150 cm and 250 cm levels.

3.6 Validation and Accuracy Assessment

The basis for evaluating the mesoform detection algorithm (SWM) was the confrontation of results with data of higher detail. To ensure the precision of the method, the obtained polygons were compared with the actual image of the channel recorded by the PlanetScope sensor. These images boast a resolution of 3.0 m, which allows for a very accurate determination of the boundaries of sandy forms. For testing, a scene was used from the day corresponding to the Sentinel-2 satellite flyover, during which the water level at the Grudziądz station was 200 cm. The entire population of objects (N=74) was verified. This means that every sandbar identified by the algorithm (after manual cleaning in the verification process) on the studied stretch of the Vistula underwent verification. All sandbars were manually digitized on the PlanetScope basemap, creating a reference layer (ground truth) for statistical comparisons. Such an approach evaluates the final statistical outcome as the true performance of the algorithm for various types of mesoforms.

The primary accuracy measure adopted in the study is the Intersection over Union (IoU) metric, which is synonymous with the Jaccard index in the literature. The choice of this metric stems from its widespread application in shape comparison tasks for arbitrary geometries (Rezatofighi et al., 2019). Unlike classic pixel statistics, IoU strictly evaluates the degree of polygon overlap while accounting for spatial shift errors and contour deformations. The index was calculated as the ratio of the area of intersection between the test and reference polygons to the area of their union:

$$IoU = \frac{|A \cap B|}{|A \cup B|} \tag{4}$$

where: A – detected polygon (Sentinel-2),
B – reference polygon (PlanetScope).

An additional validation element was checking the correlation between the total sandbar area measured by both methods. Using the coefficient of determination (R^2) allowed us to evaluate whether the difference in resolution between the two sensors led to a systematic underestimation or overestimation of the sandbar area.

4. Results

This section presents the results of the automatic detection and morphometric analysis of sandy mesoforms in the lower Vistula, obtained using the algorithm implemented in Google Earth Engine. The presented data reflect the sequence described in the methodology—from raw index extraction (SWM), through multi-stage size and manual filtration, to the final verification of result reliability against PlanetScope reference data. The results structure is divided into two main blocks:

- Analysis of extraction and filtration results, documenting the dynamics of sandbar exposure at varying water levels (from 150 to 400 cm)
- Accuracy Assessment, providing geometric and areal validation of the algorithm for a selected population of objects.
-

The following summaries allow for evaluating the method's efficiency not only statistically but also regarding limitations arising from the Sentinel-2 sensor's spatial resolution and meteorological conditions (cloud cover) during data acquisition.

4.1 Analysis of Extraction and Filtration Results

The obtained results indicate a clear inverse relationship between the water level measured at the Grudziądz gauge and the total area of exposed mesoforms. As the water level dropped from 400 cm to 150 cm, the detected area of sandbars increased from 1.7 ha to 227.5 ha. To visually illustrate this relationship, Figure 4 presents the spatio-temporal evolution of a representative sandbar alongside a 3D simulation. This 3D extrusion demonstrates the vertical dimension of the channel mesoforms relative to the gauge readings, proving how 2D satellite extractions can be translated into spatial models for relative depth calculations. The detailed results of the multi-stage identification and filtration process across different water levels are summarized in Table 3.

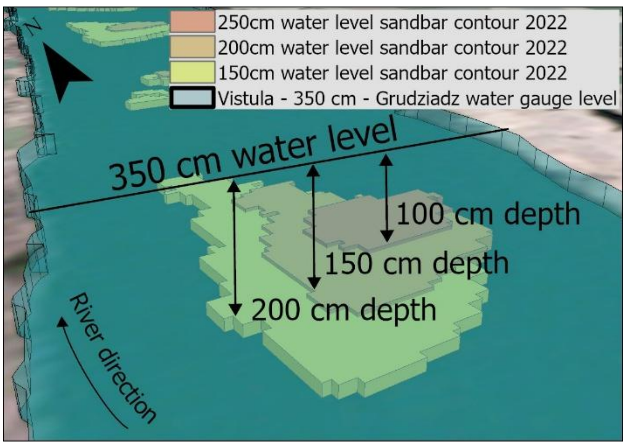

Figure 4. Spatio-temporal evolution and 3D modeling of a representative sandbar in the Lower Vistula channel.

Water Level [cm]	Acquisition Date	Cloud Cover in AOI [%]	Raw Object Count (SWM)	After Size Filtering (>1000 m²)	Final Verified Objects (N)	Total Area [ha]
400	2022-04-17	0.00%	22	14	2	1.7
350	2022-03-08	0.00%	34	20	4	1.8
300	2022-03-21	0.00%	69	50	19	11.7
250	2022-10-12	5.89%	243	142	47	46.3
200	2022-06-24	0.00%	387	231	74	157.7
150	2022-09-12	30.28%	265	159	47	227.5

Table 3. Multi-stage identification and filtration results for fluvial mesoforms (sandbars).

The multi-stage filtration process revealed a high frequency of commission errors during the raw extraction stage. For example, for the 200 cm level, the initial count of 387 raw objects was reduced to 74 verified units after applying size filtration and manual cleaning.

- Size filtration: Eliminating objects smaller than 1000 m² (10 pixels) significantly improved the structural quality of the dataset by removing spectral noise and artifacts resulting from water turbulence.
- Manual verification: The final number of verified objects (N) reflects the successful removal of anthropogenic structures (e.g., groynes and bridge supports), which possess high reflectivity similar to sand, constituting a common challenge in spatial unit detection in riverine environments.

A significant precision issue was identified for the 150 cm water level, where cloud cover in the Area of Interest (AOI) reached 30.28%. Although this date yielded the largest total area (227.5 ha), the number of detected objects (47) was lower than for the 200 cm level (74). This discrepancy stems from:

- Cloud masking: Clouds obscured smaller, isolated sandbars, leading to their exclusion from the final count,
- Incomplete observation: The reported area for this date represents only the area of effective observation, not a full channel inventory.

The 200 cm level was selected as the most reliable hydrological baseline to perform a full geometric accuracy assessment due to the complete lack of cloud cover (0.00%) and the largest population of verified, distinct spatial units (N=74).

4.2 Geometric and Area Accuracy Assessment

To verify the reliability of the automatic detection, a comparative shape analysis (polygons) was conducted for the population of N=74 mesoforms identified at the 200 cm water level. The Intersection over Union (IoU) metric was used as a measure of similarity, allowing for an evaluation of how well the results overlap with the PlanetScope reference data. Figure 5 illustrates the frequency distribution of the calculated IoU values for the validated sandbar population.

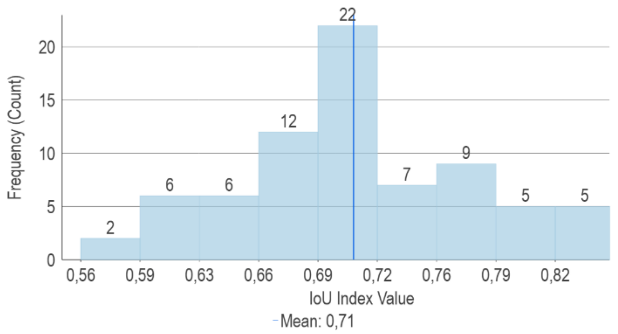

Figure 5. Histogram of the Intersection over Union (IoU) metric for the validated sandbar population (N=74) at the 200 cm water level.

The mean IoU value for the entire dataset was 0.71. This result indicates high geometric agreement, especially considering the threefold difference in spatial resolution between the compared sensors (10 m vs 3 m). The error distribution analysis showed that:

- The highest IoU values (> 0.85) were recorded for objects with a compact structure and a regular shoreline,
- Lower values (< 0.60) occurred in the case of smaller and elongated forms, where the "mixed pixel" error on the edges constituted a relatively large percentage of the total object area, and the sandbar itself extended beneath the water surface over a long distance.

The next stage of validation was checking the algorithm's stability in estimating the area of sandbars. The results were plotted on a scatter diagram (Figure 6), establishing a trend line and the coefficient of determination (R²).

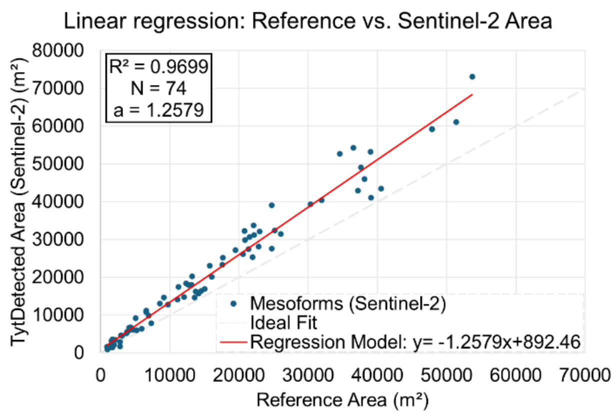

Figure 6. Linear regression comparing Sentinel-2 and PlanetScope sandbar areas.

The obtained coefficient of R^2=0.97 demonstrates an almost perfect linear relationship between the studied datasets. This proves that the SWM algorithm operates in a highly repeatable and predictable manner across the entire spectrum of mesoform sizes – from small to extensive sandy shoals. Despite high precision, the regression equation analysis revealed a systematic over-segmentation error. The slope coefficient (a = 1.26) indicates that areas determined from Sentinel-2 data are on average 26% larger than the actual reference areas. The constant offset (intercept b ≈ 892 m²) suggests that the algorithm adds a constant edge error "buffer," resulting from averaging the spectral signal in boundary pixels (water/sand).

5. Discussion

5.1 Reliability of the method in light of systematic error

The analysis of the results showed a systematic overestimation of the mesoform areas by an average of 26% (regression coefficient a = 1.26). This phenomenon directly stems from so-called boundary uncertainty and the mixed pixel effect at the water-sand interface. This occurrence is frequently encountered in remote sensing when object boundaries are not sharply defined. In the case of the Vistula, where the transition between sandy sediments and shallow water is gradual, delineating a precise outline is challenging. The primary source of this uncertainty is the spatial resolution of the utilized sensor, and for Sentinel-2 data (10 m), this error has a constant nature, yet its impact is significantly more critical for small objects than for large units (Radoux and Bogaert, 2017).

5.2 Scale effect and Mixed Pixels

The value of IoU = 0.71 and the constant area overestimation of approx. 26% directly stem from the physical limitations of the 10 m spatial resolution. At the land-water interface, Sentinel-2 pixels record a mixed signal. Because the SWM index is sensitive to the presence of sediments, these pixels are often classified as sand, causing polygons to "swell" by approx. 1-2 pixels at the edge (the so-called edge error). According to (Radoux and Bogaert, 2017) observations in object-based image analysis (GEOBIA), these errors are unavoidable when transitioning to a lower resolution, but their impact diminishes as the object size increases. This is confirmed by the obtained results—the largest sandbars, despite a large absolute error, exhibit the highest structural cohesion.

5.3 Navigational implications

The systematic error identified in the study, manifesting as a 26 percent surface addition, acts as a conservative safety buffer. In inland navigation, where the priority is avoiding the underestimation of channel obstacles, the tendency to over-segment sandbar boundaries is a desirable trait, provided it is explicitly reported. Reliable documentation of such sources of uncertainty is a necessary condition for the proper use of cartographic products and their correct interpretation by end-users (Radoux and Bogaert, 2017). Since in wall-to-wall maps the rank of a given object is proportional to its surface area, the high detection stability of the largest mesoforms ($R^2 = 0.97$) guarantees the provision of reliable information regarding obstacles of the highest importance to route navigability.

Furthermore, by establishing the exact water gauge level at which specific sandbars emerge, the proposed method allows for the calculation of the available water column over these obstacles during higher water stages. For instance, if a sandbar is mapped as exposed at a 150 cm water level, a navigator can deduce that at a current gauge reading of 400 cm, there is a theoretical 2.5-meter water column (250 cm) above that specific obstacle. However, this theoretical column is not synonymous with the maximum permissible vessel draft. To assess actual navigability, the vessel's specific draft and the mandatory under-keel clearance (UKC) must be factored into this available water depth. Additionally, when applying this differential logic in real-time, the hydrological time lag (wave propagation delay) must be strictly accounted for. A dynamic change in the water level at the Grudziądz gauge will not manifest instantaneously across the entire 55-kilometer downstream stretch. Consequently, to avoid dangerous depth miscalculations and grounding, end-users and RIS systems must incorporate both the vessel's draft parameters and the water wave travel time to accurately correlate the current gauge reading with the local navigable depth.

The use of free Sentinel-2 data and automation within the Google Earth Engine environment unlocks the potential for conducting cyclic, annual monitoring of the Vistula's morphodynamics, which is essential for the comparability of research results over long time series. However, a significant operational limitation must be noted, namely the impact of meteorological conditions on dataset completeness. In remote sensing practice, acquiring information that exhaustively covers the study area at every desired time is often impossible, e.g., due to cloud cover. From the perspective of navigation safety, this means that a lack of sandbar detection during periods of incomplete visibility cannot be interpreted as confirmation of a clear navigable route, but rather as an error stemming from limitations in the sensor's spectral response. Awareness of these "visibility masks" coupled with the surface stability of the algorithm allows raw satellite data to be transformed into a reliable tool supporting river navigation.

6. Conclusions

The analysis of the results of automated sandbar detection in the Vistula channel allows for the formulation of the following conclusions:

- The use of Sentinel-2 data and the Google Earth Engine platform enables repeatable, annual inventories of channel obstacles on a river-wide scale. This method provides a low-cost supplement to traditional bathymetric measurements,
- The algorithm exhibits high stability in estimating the total sandbar area ($R^2 = 0.97$), with a simultaneous systematic overestimation of their size by 26%. This error stems from the sensor's resolution (10 m) and boundary uncertainty at the water-sediment interface.
- The observed area surplus serves as a conservative safety margin. From a navigational perspective, overestimating the boundaries of shoals is safer than underestimating them. However, this requires explicit reporting of the edge error, which may artificially narrow the route on the map.
- During periods of high river energy (e.g., surges, floods), when sediment migration accelerates, it is necessary to shorten the image selection period (temporal windowing). This will reduce errors arising from sandbar displacement during data acquisition, even at the cost of lesser water level consistency at the gauge.
- The primary limit of the method remains optical data gaps caused by cloud cover. The failure to detect an object under such conditions must be reported as "no data" and not as confirmation of a clear navigable route.

Future research should focus on integrating optical data with radar imagery (SAR) to eliminate the impact of cloud cover, and on automating dynamic time window selection during periods of high hydrological dynamics. A promising direction is also the development of a mobile interface for end-users (helmsmen) that would integrate up-to-date channel clearance maps with positioning systems (GNSS) via web services (WMS/WFS). Crucially, to ensure safe dynamic relative depth mapping, such River Information Services (RIS) must incorporate hydrodynamic routing to account for the wave propagation delay (hydrological time lag) between the reference gauge and the vessel's current downstream position.

References

Babiński, Z., 1992. WSPÓŁCZESNE PROCESY KORYTOWE DOLNEJ WISŁY.

Habel, M., 2018. Effects of flow regulation and river channelization on sandbar bird nesting availability at the Lower Vistula River. Ecological Questions 29, 43–53. https://doi.org/10.12775/EQ.2018.028

Habel, M., 2013. Dynamic of Vistula River channel deformations downstream of Włocławek Reservoir. https://doi.org/10.13140/2.1.4606.0803

Head Office of Geodesy and Cartography (GUGiK), 2025. Topographic Objects Database [Baza Danych Obiektów Topograficznych BDOT10K].

Institute of Meteorology and Water Management - National Research Institute, 2022. Public Information Bulletin - Hydrological and Meteorological Data [Biuletyn Informacji Publicznej - Dane Hydrologiczno-Meteorologiczne] [WWW Document]. IMGW-PIB Public Data Service. URL https://danepubliczne.imgw.pl/ (accessed 3.21.26).

Kotowska, I., Mańkowska, M., Pluciński, M., 2019. Planning the development of inland shipping in the seaport- hinterland transport: A case study of the Oder River in Poland 84–92. https://doi.org/10.17402/340

Kryniecka, K., Magnuszewski, A., 2021. Application of Satellite Sentinel-2 Images to Study Alternate Sandbars Movement at Lower Vistula River (Poland). Remote Sensing 13. https://doi.org/10.3390/rs13081505

Kryniecka, K.O., Magnuszewski, A., 2020. Use of Sentinel-2 images for the detection of sandbars along the Lower Vistula. Acta Sci. Pol. Formatio Circumiectus 19, 23–33. https://doi.org/10.15576/ASP.FC/2020.19.2.23

Kubiak-Wójcicka, K., Manoiu, V.-M., 2025. International Inland Waterways in Poland: Current State and Their Importance in EU Transport Policy. Water 17. https://doi.org/10.3390/w17223190

Monitoring Hydro - Hydrological Service of Poland [Serwis Hydrologiczny - Monitoring Hydro], 2026. Monitoring Hydro - Hydrological Service of Poland [Serwis Hydrologiczny - Monitoring Hydro] [WWW Document]. Institute of Meteorology and Water Management - National Research Institute. URL https://hydro.imgw.pl/ (accessed 3.21.26).

Office of the Marshal of the Pomorskie Voivodeship, 2026. The Vistula River - International Waterway E70 [WWW Document]. International Waterway E70. URL https://mdwe70.pl/en/waterways/waterbodies/the-vistula-river/ (accessed 3.17.26).

Pieron, Ł., Hojan, M., Habel, M., 2013. Charakterystyka łach korytowych uregulowanego odcinka Dolnej Wisły.

Prime Minister, 2022. Announcement of the Prime Minister on the uniform text of the Regulation on the classification of inland waterways [Obwieszczenie w sprawie ogłoszenia jednolitego tekstu rozporządzenia w sprawie klasyfikacji śródlądowych dróg wodnych], Journal of Laws [Dziennik Ustaw].

Radoux, J., Bogaert, P., 2017. Good Practices for Object-Based Accuracy Assessment. Remote Sensing 9, 646. https://doi.org/10.3390/rs9070646

Rezatofighi, H., Tsoi, N., Gwak, J., Sadeghian, A., Reid, I., Savarese, S., 2019. Generalized Intersection Over Union: A Metric and a Loss for Bounding Box Regression, in: 2019 IEEE/CVF Conference on Computer Vision and Pattern Recognition (CVPR). Presented at the 2019 IEEE/CVF Conference on Computer Vision and Pattern Recognition (CVPR), pp. 658–666. https://doi.org/10.1109/CVPR.2019.00075

Schoeneich, M., Habel, M., Szatten, D., Absalon, D., Montewka, J., 2022. An Integrated Approach to an Assessment of Bottlenecks for Navigation on Riverine Waterways. https://doi.org/10.3390/w15010141

Sentinel-2 Products Specification Document [WWW Document], 2025. URL https://sentiwiki.copernicus.eu/web/document-library#DocumentLibrary-SENTINEL-2DocumentsLibrary-S2-Documents

Technical Specification | Planet Documentation [WWW Document], 2026. URL https://docs.planet.com/data/imagery/planetscope/techspec/ (accessed 3.21.26).

Woś, K., 2017. PLANS FOR THE DEVELOPMENT OF POLISH INLAND WATERWAYS. Zeszyty Naukowe Uniwersytetu Szczecińskiego Problemy Transportu i Logistyki 37, 297–310. https://doi.org/10.18276/ptl.2017.37-37